



# Hybrid Improper Ferroelectricity in Columnar (NaY)MnMnTi<sub>4</sub>O<sub>12</sub>

Rebecca Scatena,\* Ran Liu, Vladimir V. Shvartsman, Dmitry D. Khalyavin,  
 Yoshiyuki Inaguma, Kazunari Yamaura, Alexei A. Belik, and Roger D. Johnson

**Abstract:** We show that cation ordering on A site columns, oppositely displaced via coupling to B site octahedral tilts, results in a polar phase of the columnar perovskite (NaY)MnMnTi<sub>4</sub>O<sub>12</sub>. This scheme is similar to hybrid improper ferroelectricity found in layered perovskites, and can be considered a realisation of hybrid improper ferroelectricity in columnar perovskites. The cation ordering is controlled by annealing temperature and when present it also polarises the local dipoles associated with pseudo-Jahn–Teller active Mn<sup>2+</sup> ions to establish an additional ferroelectric order out of an otherwise disordered dipolar glass. Below T<sub>N</sub> ≈ 12 K, Mn<sup>2+</sup> spins order, making the columnar perovskites rare systems in which ordered electric and magnetic dipoles may reside on the same transition metal sublattice.

The study of ferroelectricity in perovskite-type oxides is now more prominent than ever following the boom in fundamental and applied research into multiferroic materials.<sup>[1–4]</sup> While proper ferroelectric instabilities typically originate in *pseudo*-Jahn–Teller (*pJT*) d<sup>0</sup> covalency (e.g. Ti<sup>4+</sup>)<sup>[5]</sup> or stereochemical lone-pair activity (e.g. Pb<sup>2+</sup> or Bi<sup>3+</sup>),<sup>[6,7]</sup> the perovskite framework has the potential to support more exotic mechanisms of electric polarisation. The so-called GdFeO<sub>3</sub> distortion<sup>[8]</sup> is ubiquitous in ABO<sub>3</sub> simple perovskites and can be understood in terms of antiphase BO<sub>6</sub> octahedral rotations within the *ab*-plane, accompanied by in-phase octahedral rotations about the *c*-axis; (a<sup>−</sup>, a<sup>−</sup>, c<sup>+</sup>) in Glazer notation.<sup>[9]</sup> These rotations together introduce displacements of A site cations that are exactly

opposite in direction from one layer to the next on moving along *c*. If alternate layers are made symmetry inequivalent a net polarisation may be established, as is the case for some Ruddlesden–Popper<sup>[10]</sup> and Dion–Jacobson<sup>[11]</sup> phases, or composite heterostructures.<sup>[12,13]</sup> This form of electric polarisation, known as hybrid improper ferroelectricity, was demonstrated relatively recently and has generated new directions in ferroelectrics and multiferroics research.<sup>[14]</sup>

In this communication, we go beyond the layered paradigm of hybrid improper ferroelectricity and demonstrate that a similar phenomenon can be activated in the columnar perovskite (NaY)MnMnTi<sub>4</sub>O<sub>12</sub> (general formula A<sub>2</sub>A'A''B<sub>4</sub>O<sub>12</sub>). In this material Na<sup>+</sup> and Y<sup>3+</sup> ions are distributed over oppositely displaced A site columns established by an (a<sup>+</sup>, a<sup>+</sup>, c<sup>−</sup>) octahedral tilting scheme, in contrast to the oppositely displaced *layers* discussed above. Mn<sup>2+</sup> ions are found in square-planar (A') and tetrahedral (A'') sites, while Ti<sup>4+</sup> ions are located at the perovskite B sites.<sup>[15]</sup> We show that a partial ordering of Na<sup>+</sup> and Y<sup>3+</sup> between the oppositely displaced columns can be controlled by the annealing temperature, and stabilised to generate a hybrid improper polarisation. (NaY)MnMnTi<sub>4</sub>O<sub>12</sub> also supports a *pJT* ferroelectric instability associated with underbonded, square-planar coordinated Mn<sup>2+</sup> ions as found in CaMnTi<sub>2</sub>O<sub>6</sub>.<sup>[16,17]</sup> We show that in the absence of A site cation order the *pJT* instability leads to a globally centrosymmetric Mn<sup>2+</sup> dipolar-glass, while in the presence of A site cation order a Mn<sup>2+</sup> proper ferroelectric polarisation is established. Finally, we show that antiferromagnetic order of the same Mn<sup>2+</sup> ions develops in both structures below T<sub>N</sub> = 12 K.

[\*] Dr. R. Scatena

Department of Physics, Clarendon Laboratory, University of Oxford  
 Parks Road, Oxford, OX1 3PU (UK)  
 E-mail: rebecca.scatena@physics.ox.ac.uk

Dr. R. Scatena, Dr. R. D. Johnson  
 Department of Physics and Astronomy, University College London  
 Gower Street, London, WC1E 6BT (UK)

Dr. R. Liu, Dr. K. Yamaura, Dr. A. A. Belik  
 Research Center for Materials Nanoarchitectonics (MANA), National Institute for Materials Science (NIMS)  
 Namiki 1-1, Tsukuba, Ibaraki 305-0044 (Japan)

Dr. R. Liu, Dr. K. Yamaura  
 Graduate School of Chemical Sciences and Engineering, Hokkaido University  
 North 10 West 8, Kita-ku, Sapporo, Hokkaido 060-0810 (Japan)

Dr. V. V. Shvartsman

Institute for Materials Science and CENIDE—Centre for Nano-integration Duisburg-Essen, University of Duisburg-Essen  
 45141 Essen (Germany)

Dr. D. D. Khalyavin  
 ISIS Facility, Rutherford Appleton Laboratory  
 Didcot, OX11 0QX (UK)

Dr. Y. Inaguma  
 Department of Chemistry, Faculty of Science, Gakushuin University  
 1-5-1 Mejiro, Toshima-ku, Tokyo 171-8588 (Japan)

© 2023 The Authors. Angewandte Chemie International Edition published by Wiley-VCH GmbH. This is an open access article under the terms of the Creative Commons Attribution Non-Commercial NoDerivs License, which permits use and distribution in any medium, provided the original work is properly cited, the use is non-commercial and no modifications or adaptations are made.

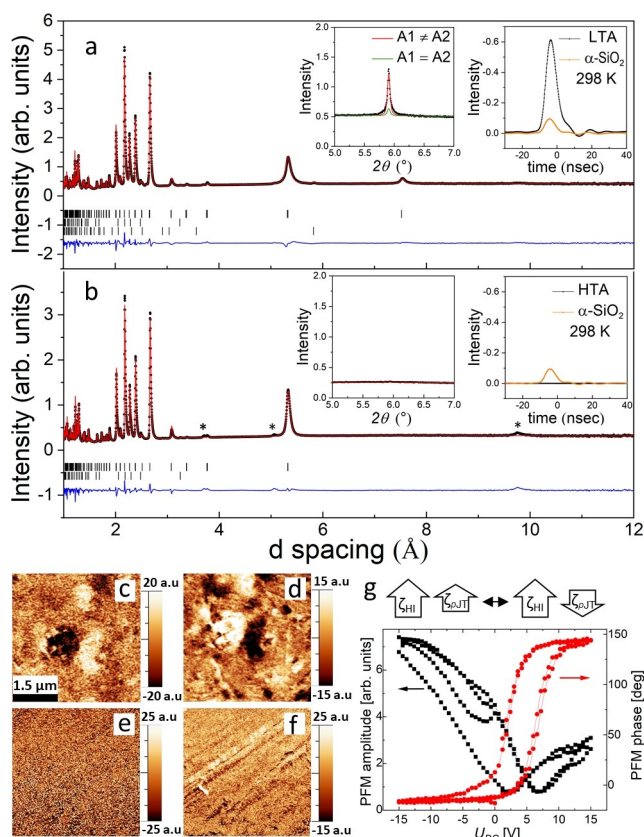


**Figure 1.** Experimental (black dots), calculated (red line) and difference (blue line) NPD patterns of a) sample LTA and b) sample HTA of  $(\text{NaY})\text{MnMnTi}_4\text{O}_{12}$  at 100 K. Tick marks show Bragg reflection positions for the main perovskite phase (first row),  $\text{TiO}_2$  impurity (second row) and  $\text{Y}_2\text{Ti}_2\text{O}_7$  (third row). Asterisks mark peaks belonging to an unidentified impurity phase. Insets: {100} peak region measured by PXRD where A1 and A2 are the columns in the structure (left) and SHG measured at 298 K (right). Vertical and lateral PFM images are shown in c), and d) for sample LTA, and in e) and f) for sample HTA. Panel g) shows a local piezoresponse hysteresis loop.

Two polycrystalline samples of  $(\text{NaY})\text{MnMnTi}_4\text{O}_{12}$  with the same nominal composition were prepared from stoichiometric mixtures of  $\text{MnO}$ , “ $\text{Na}_2\text{TiO}_3$ ” (a mixture of  $\beta\text{-Na}_2\text{TiO}_3$  and  $\text{Na}_8\text{Ti}_5\text{O}_{12}$ ),  $\text{Y}_2\text{O}_3$  and  $\text{TiO}_2$  at 6 GPa using a belt-type high-pressure apparatus (Supporting Information). One sample was annealed at 1550 K (labeled LTA for low-T annealing), and the other was annealed at 1750 K (labeled HTA for high-T annealing). The 100 K crystal structure of both samples was characterised by synchrotron powder X-ray diffraction (PXRD) performed at beamline BL02B2 of SPring-8, Japan,<sup>[18,19]</sup> and by neutron powder diffraction (NPD) using the WISH instrument<sup>[20]</sup> at ISIS, UK.

The PXRD and NPD data from sample LTA (Figure 1a) could be fitted by a main phase with the columnar perovskite parent symmetry of  $P4_2/nmc$ <sup>[21]</sup> (Figure 2a), plus trace  $\text{TiO}_2$  and  $\text{Y}_2\text{Ti}_2\text{O}_7$  impurity phases. In addition, a weak {100} family of reflections, indexed with respect to the main phase but forbidden by the  $n$ -glide was clearly observed (Figure 1a left inset). Hence, the symmetry of sample LTA could be no higher than the polar space group  $P4_2mc$ , as found for the proper ferroelectric  $\text{CaMnTi}_2\text{O}_6$ .<sup>[16]</sup> The assignment of a polar space group to sample LTA was confirmed by second-harmonic-generation (SHG) measurements (Figure 1a right inset, see Supporting Information for details) and the observation of piezoelectric activity in RT piezoresponse force microscopy (PFM). The dark and light regions in the PFM images (Figure 1c and d) revealed the presence of domains with opposite polarity, and the piezoresponse induced by a dc electric field (Figure 1g) demonstrated strongly asymmetric hysteretic polarization switching.

The atomic displacements that contribute towards the ferroelectric polarization in  $P4_2mc$  symmetry occur parallel to the  $c$ -axis.<sup>[16]</sup> One can show that such displacements give zero diffraction intensity at the {100} Bragg positions. Instead, the {100} intensity may originate in displacements of  $\text{Ti}^{4+}$  and/or  $\text{O}^{2-}$  ions within the  $ab$ -plane, and/or a degree of  $\text{Na}^+/\text{Y}^{3+}$  cation ordering between two A site sublattices

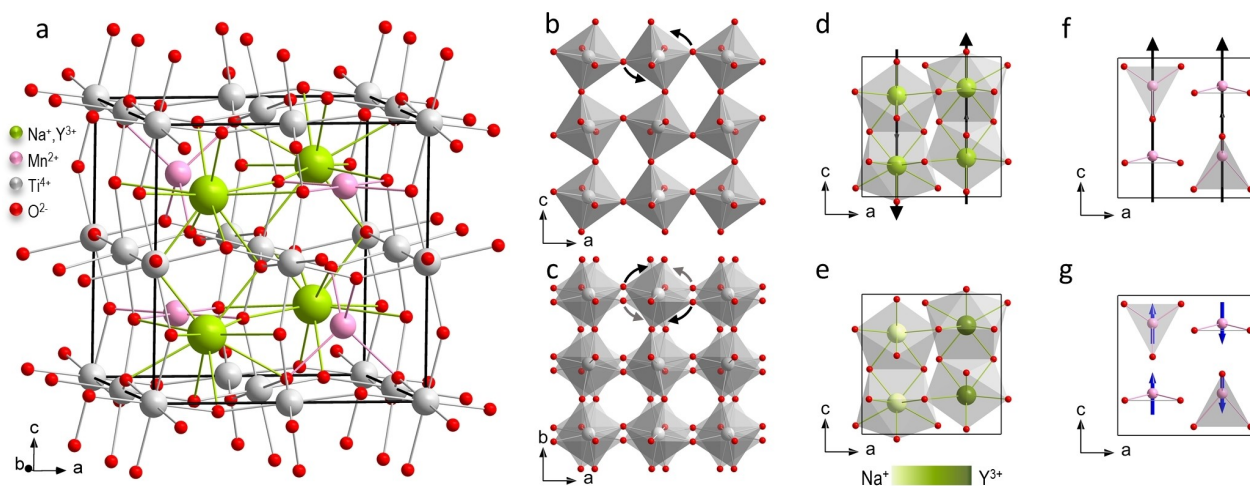


**Figure 2.** a) Crystal structure of  $(\text{NaY})\text{MnMnTi}_4\text{O}_{12}$ , b)  $(a^+, a^+, 0)$  octahedra tilts ( $A_4^+$  irrep), c)  $(0, 0, c^-)$  octahedra tilts ( $Z_2^-$  irrep), d) columnar shifts ( $M_3^-$  irrep), e) cation ordering ( $M_1^+$  irrep), f) proper polar distortions ( $\Gamma_3^-$  irrep) and g) C-type magnetic structure.

that become inequivalent in  $P4_2mc$  (Wyckoff sites 2a and 2b). To disentangle these two structural modifications we performed a joint refinement against PXRD and NPD data using FULLPROF,<sup>[22]</sup> exploiting the different sensitivity of the X-ray and neutron scattering amplitudes to  $Ti^{4+}/O^{2-}$  displacements and ordering of  $Na^+$  and  $Y^{3+}$  (Supporting Information). We obtained a structural model in which  $Ti^{4+}/O^{2-}$  displacements were minimal, but with a significant degree of  $Na^+$  and  $Y^{3+}$  cation ordering ( $\approx 25\%$ ) that maintained the  $Na^+/Y^{3+}$  compositional ratio of 1:1. Analysis of  $(NaY)-O$  bond lengths showed that the partial cation ordering was accompanied by contractions and expansions of the local oxygen coordination spheres consistent with the different cation radii. The refined structural model also included substantial ordered polar displacements of  $A' Mn^{2+}$  ions parallel to the  $c$ -axis. This additional contribution to the macroscopic polarization implies the possibility of partial switching under external electric field; a likely origin of the hysteresis loop asymmetry observed in our PFM measurements (Figure 1g). The polar phase of sample LTA was found to persist up to 1070 K—close to the expected decomposition temperature—with no evidence for a polar to centrosymmetric phase transition at high temperature (Supporting Information).

In contrast, the  $\{100\}$  peak was absent in PXRD and NPD patterns collected from sample HTA (Figure 1b) indicating a centrosymmetric  $P4_2/nmc$  crystal structure for the main phase. This space group assignment was confirmed by SHG and PFM, which showed no measurable intensity (Figure 1b right inset) or piezoelectric activity (Figure 1e and f), respectively. Joint refinement of a  $P4_2/nmc$  structural model against the X-ray and neutron data confirmed a 1:1 ratio of  $Na^+$  and  $Y^{3+}$  cations statistically distributed across the symmetry equivalent A-sites. The  $A' Mn^{2+}$  cations had an unphysically large isotropic thermal parameter, and a better fit could be achieved by including positional disorder above and below the square planar coordination. These disordered  $A' Mn^{2+}$  displacements break local inversion symmetry, and hence represent a proper ferroelectric instability. While in sample LTA cooperative ferroelectric order has emerged, the HTA sample maintains a disordered dipolar-glass-like state at the  $A'$  site.

To explore symmetry relations and coupling schemes between structural distortions, we used a higher symmetry parent tetragonal structure with space group  $P4/mmm$  that has the same atomic connectivity as both  $P4_2/nmc$  and  $P4_2mc$  structures (Figure 2) but with octahedral rotations and columnar shifts removed (Supporting Information). From decomposition of the polar  $P4_2mc$  structure with respect to symmetry adapted distortion modes of the parent<sup>[23]</sup> (Supporting Information) we identified a trilinear free energy invariant of the form  $\eta_1\eta_2\epsilon$ , which describes the stabilization of alternating A-site columnar shifts ( $\epsilon$ ) by large octahedral tilt modes ( $\eta_1, \eta_2$ ) (see Figure 2). One can show that this coupling is also present in the centrosymmetric  $P4_2/nmc$  symmetry, and it is analogous to the alternating shifts of A-site layers induced by octahedral tilts in  $ABX_3$  perovskites. Our analysis found another trilinear invariant of the form  $\zeta_{HI}\delta\epsilon$  (Supporting Information), which generates

hybrid improper ferroelectricity ( $\zeta_{HI}$ ) by A-site cation ordering ( $\delta$ ) coupled to the columnar shifts ( $\epsilon$ )—again in close analogy to hybrid improper ferroelectricity in the layered systems. Finally, one can identify a bilinear invariant of the form  $\zeta_{HI}\zeta_{pJT}$  that directly couples the pJT instability associated with the  $A' Mn^{2+}$  ions to the hybrid improper ferroelectric polarisation, hence stabilising additional improper ferroelectric order out of an otherwise disordered  $Mn^{2+}$  dipolar glass.

The magnetic susceptibilities of both samples indicate phase transitions to an antiferromagnetic (AFM) ground state below  $T_N=12$  K (Figure 3 left insets). For both samples, variable temperature NPD data showed magnetic intensities developing below  $T_N$  at Bragg positions that uniquely identify AFM layers stacked ferromagnetically along  $c$  (Figure 2g). A very weak magnetic intensity was measured at  $\{111\}$ , which implied different size moments on the  $A'$  and  $A''$  sites. This magnetic structure (magnetic space groups  $P4_2'/n'm'c$  (No. 137.512) and  $P4_2'm'c$  (No. 105.213) for the non-polar and polar structures, respectively) was refined against NPD data collected at 1.5 K, as shown in Figure 3, where the temperature evolution of the refined magnetic moments is shown in the right insets.

In summary, we have shown that  $Na^+/Y^{3+}$  cation order in  $(NaY)MnMnTi_4O_{12}$  can be introduced on A site columns oppositely displaced by B site octahedral tilts, resulting in an emergent polar phase in direct analogy to layered hybrid improper ferroelectrics. The hybrid improper ferroelectricity in  $(NaY)MnMnTi_4O_{12}$  couples to a second polar instability of the  $Mn^{2+}$  ions, which develops additional ferroelectric

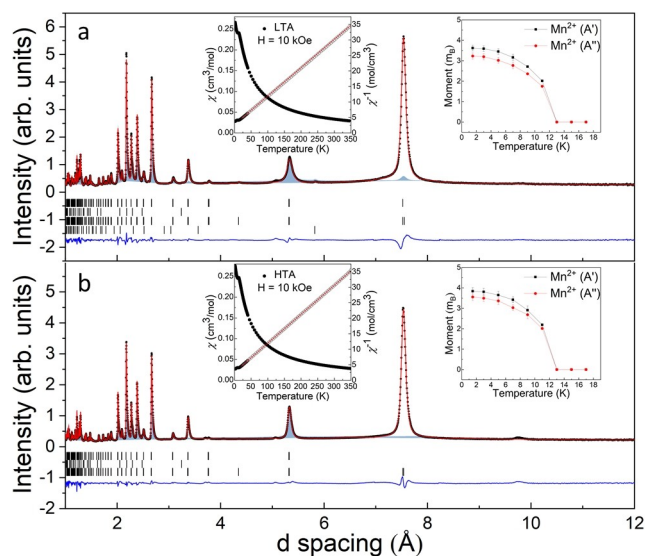


**Figure 3.** Experimental (black dots), calculated (red line) and difference (blue line) NPD patterns of a) sample LTA and b) sample HTA of  $(NaY)MnMnTi_4O_{12}$  at 1.5 K. Light blue shading shows the nuclear contribution to the Bragg intensities. Tick marks show Bragg reflection positions for the main perovskite phase (first row),  $TiO_2$  impurity (second row), C-type  $Mn^{2+}$  magnetic structure (third row) and  $Y_2Ti_2O_7$  (forth row). Insets: (left) DC magnetic susceptibility  $\chi$  and Curie–Weiss fitted  $\chi^{-1}$  versus T curves and (right) temperature dependence of the ordered magnetic moments.

order out of an otherwise disordered dipolar glass, giving rise to asymmetric electric field switching of the net electric polarisation. We note that the presence of unpaired d-electrons and the respective magnetic moment is typically assumed to reduce the tendency for pJT ferroelectric distortions,<sup>[24]</sup> yet we show that the Mn<sup>2+</sup> ions adopt long range antiferromagnetic order below 12 K. Hence, the polar (NaY)MnMnTi<sub>4</sub>O<sub>12</sub> perovskite presents a rare case in which ordered electric and magnetic dipoles reside on the same transition metal sublattice, opening a new route to combining ferroelectric and magnetic orders in the solid state. The columnar perovskite framework provides great chemical flexibility, and one might anticipate a number of materials similar to (NaY)MnMnTi<sub>4</sub>O<sub>12</sub> that can realise hybrid improper ferroelectricity with cross-coupled polar instabilities intimately related to magnetism.

### Acknowledgements

The synchrotron radiation experiments were performed at SPring-8 with the approval of the Japan Synchrotron Radiation Research Institute (Proposal Nos. 2021A1169 and 2021A1334). We thank Dr. S. Kobayashi for his assistance at SPring-8 and Dr. Y. Matsushita for his help with HT XRD. R.D.J. acknowledges support from a Royal Society University Research Fellowship. R.S. acknowledges support from the Swiss National Science Foundation (P2BEP2-188253). A.A.B. and K.Y. acknowledge support from Grant-in-Aid for Scientific Research from the Japan Society for the Promotion of Science (No. JP22H04601) and the Kazuchika Okura Memorial Foundation (No. 2022-11). MANA is supported by World Premier International Research Center Initiative (WPI), MEXT, Japan.

### Conflict of Interest

The authors declare no conflict of interest.

### Data Availability Statement

The data that support the findings of this study are available in the Supporting Information of this article.

**Keywords:** Columnar Perovskites · Ferroelectrics · Hybrid Improper Ferroelectricity · Multiferroics · Perovskite

- [1] W. Eerenstein, N. D. Mathur, J. F. Scott, *Nature* **2006**, *442*, 759–765.
- [2] S. W. Cheong, M. Mostovoy, *Nat. Mater.* **2007**, *6*, 13–20.
- [3] K. F. Wang, J. M. Liu, Z. F. Ren, *Adv. Phys.* **2009**, *58*, 321–448.
- [4] D. Khomskii, *Physics* **2009**, *2*, 20.
- [5] I. B. Bersuker, *Chem. Rev.* **2013**, *113*, 1351–1390.
- [6] T. Abe, S. Kim, C. Moriyoshi, Y. Kitanaka, Y. Noguchi, H. Tanaka, Y. Kuroiwa, *Appl. Phys. Lett.* **2020**, *117*, 252905.
- [7] D. D. Khalyavin, R. D. Johnson, F. Orlandi, P. G. Radaelli, P. Manuel, A. A. Belik, *Science* **2020**, *369*, 680–684.
- [8] S. Geller, *J. Chem. Phys.* **1956**, *24*, 1236.
- [9] A. M. Glazer, *Acta Crystallogr. Sect. B* **1972**, *28*, 3384–3392.
- [10] S. Mallick, A. D. Fortes, W. Zhang, P. S. Halasyamani, M. A. Hayward, *Chem. Mater.* **2021**, *33*, 2666–2672.
- [11] N. A. Benedek, *Inorg. Chem.* **2014**, *53*, 3769–3777.
- [12] C.-G. Duan, S. S. Jaswal, E. Y. Tsybmal, *Phys. Rev. Lett.* **2006**, *97*, 047201.
- [13] J. M. Rondinelli, M. Stengel, N. A. Spaldin, *Nat. Nanotechnol.* **2007**, *2*, 46–50.
- [14] N. A. Benedek, C. J. Fennie, *Phys. Rev. Lett.* **2011**, *106*, 107204.
- [15] A. A. Belik, *Dalton Trans.* **2018**, *47*, 3209–3217.
- [16] A. Aimi, D. Mori, K. I. Hiraki, T. Takahashi, Y. J. Shan, Y. Shirako, J. Zhou, Y. Inaguma, *Chem. Mater.* **2014**, *26*, 2601–2608.
- [17] G. Gou, N. Charles, J. Shi, J. M. Rondinelli, *Inorg. Chem.* **2017**, *56*, 11854–11861.
- [18] S. Kawaguchi, M. Takemoto, K. Osaka, E. Nishibori, C. Moriyoshi, Y. Kubota, Y. Kuroiwa, K. Sugimoto, *Rev. Sci. Instrum.* **2017**, *88*, 085111.
- [19] S. Kawaguchi, M. Takemoto, H. Tanaka, S. Hiraide, K. Sugimoto, Y. Kubota, *Journal of Synchrotron Radiation* **2020**, *27*, 616–624.
- [20] L. C. Chapon, P. Manuel, P. G. Radaelli, C. Benson, L. Perrott, S. Ansell, N. J. Rhodes, D. Raspino, D. Duxbury, E. Spill, J. Norris, *Neutron News* **2011**, *22*, 22–25.
- [21] R. Liu, R. Scatena, D. D. Khalyavin, R. D. Johnson, Y. Inaguma, M. Tanaka, Y. Matsushita, K. Yamaura, A. A. Belik, *Inorg. Chem.* **2020**, *59*, 9065–9076.
- [22] J. Rodríguez-Carvajal, *Phys. Rev. B* **1993**, *192*, 55–69.
- [23] B. J. Campbell, H. T. Stokes, D. E. Tanner, D. M. Hatch, *J. Appl. Crystallogr.* **2006**, *39*, 607–614.
- [24] N. A. Hill, *J. Phys. Chem. B* **2000**, *104*, 6694–6709.
- [25] Deposition Numbers 2263015 and 2263016 contains the supplementary crystallographic data for this paper. These data are provided free of charge by the joint Cambridge Crystallographic Data Centre and Fachinformationszentrum Karlsruhe Access Structures service.

Manuscript received: April 28, 2023

Accepted manuscript online: May 18, 2023

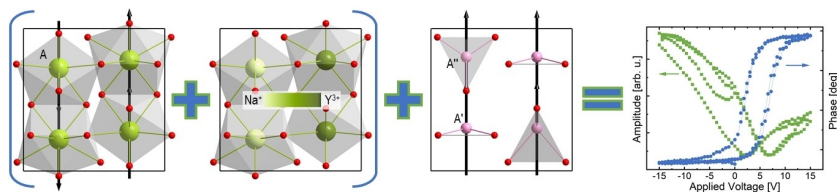
Version of record online: ■■■, ■■■

## Communications

## Perovskite Ferroelectrics

R. Scatena,\* R. Liu, V. V. Shvartsman,  
D. D. Khalyavin, Y. Inaguma, K. Yamaura,  
A. A. Belik, R. D. Johnson — e202305994

Hybrid Improper Ferroelectricity in Columnar  
(NaY)MnMnTi<sub>4</sub>O<sub>12</sub>



In columnar order quadrupole perovskites  $A_2A'A''B_4O_{12}$  hybrid improper ferroelectricity emerges through A-site cation ordering across anti-displaced structural columns. This novel form of polar order couples to an intrinsic

proper ferroelectric instability associated with underbonded magnetic  $A' Mn^{2+}$  ions, giving rise to a biased, asymmetric switching response under applied electric field that coexists at low temperature with antiferromagnetism.